Research Square

Preprints are preliminary reports that have not undergone peer review.
They should not be considered conclusive, used to inform clinical practice,
or referenced by the media as validated information.

Histopathological, Hematological and Coagulation Disturbances Induced by Macrovipera lebetina obtusa Envenomation: Evaluation of Experimental Inhibitors

Arsen Kishmiryan
Orbeli Institute of Physiology, National Academy of Sciences of the Republic of Armenia
Gevorg Avagyan
drgevavagyan@gmail.com

Yerevan State University
Vardan Dabaghyan
Yerevan State Medical University
Heghine Khachatryan
Yeolyan Hematology and Oncology Center
Ashot Aslanyan
Orbeli Institute of Physiology, National Academy of Sciences of the Republic of Armenia
Naira Ayvazyan
Orbeli Institute of Physiology, National Academy of Sciences of the Republic of Armenia

Research Article

Keywords: snakebite envenomation, Macrovipera lebetina obtusa, hematology, coagulopathy, histopathology, marimastat, varespladib, enzyme inhibitors

Posted Date: November 19th, 2026

DOI: https://doi.org/10.21203/rs.3.rs-9599317/v1

License: This work is licensed under a Creative Commons Attribution 4.0 International License.
Read Full License

Additional Declarations: No competing interests reported.

Histopathological, Hematological and Coagulation Disturbances Induced by *Macrovipera lebetina obtusa* Envenomation: Evaluation of Experimental Inhibitors

Abstract

Background: Snakebite envenomation caused by *Macrovipera lebetina obtusa* represents a significant medical problem due to its hemotoxic effects and ability to induce systemic coagulopathy and multi-organ damage. This study investigated hematological, coagulation, and histopathological alterations induced by its venom and evaluated the effects of the enzyme inhibitors marimastat and varespladib.

Methods: Experimental models were established in rats and mice using venom alone or venom pre-incubated with inhibitors. Hematological, coagulation and histopathological parameters were assessed.

Results: Venom exposure resulted in pronounced hemoconcentration, reflected by increased erythrocyte count, hemoglobin and hematocrit levels, likely due to increased vascular permeability and plasma leakage. Coagulation disturbances were primarily characterized by prolongation of the prothrombin time and elevation of the international normalized ratio, while the activated partial thromboplastin time remained largely unchanged. Histopathological analysis revealed severe hemorrhagic and structural alterations across multiple organs, including the heart, lung, liver, and kidney. Pre-incubation with marimastat partially attenuated these effects, reducing vascular damage, hemoconcentration, and coagulation abnormalities, whereas varespladib demonstrated more limited protective efficacy, with persistent tissue injury and coagulation disturbances. Animals receiving inhibitor-treated venom survived up to 7 days, indicating reduced acute toxicity.

Conclusions: These findings demonstrate that *Macrovipera lebetina obtusa* venom induces complex systemic toxicity mediated by multiple toxin families, and that inhibition of metalloproteinases provides greater protection than inhibition of phospholipase A_2. However, the pre-

incubation model does not fully reflect clinical envenomation, and the results support the need for multi-target therapeutic strategies to effectively neutralize venom-induced pathology.

Keywords: snakebite envenomation, *Macrovipera lebetina obtusa,* hematology, coagulopathy, histopathology, marimastat, varespladib, enzyme inhibitors

Introduction

Snakebite envenomation remains a major global public health problem, particularly in tropical and subtropical regions, where it contributes substantially to morbidity, mortality, and long-term disability. The World Health Organization estimates that more than five million snakebites occur annually worldwide, leading to approximately 2.7 million envenomations and between 81,000 and 138,000 deaths each year [1, 2]. In addition to mortality, many survivors suffer permanent disabilities, including amputations and severe tissue damage. Because of its substantial health burden, snakebite envenoming has been recognized by the World Health Organization as a neglected tropical disease requiring urgent global attention [3].

Viperid snakes are among the most clinically important causes of envenomation due to the potent hemotoxic and tissue-destructive properties of their venoms. The blunt-nosed viper, *Macrovipera lebetina obtusa*, represents one of the most medically significant venomous species in the South Caucasus and Middle Eastern regions. This species has a wide geographical distribution and is frequently encountered near human settlements, increasing the likelihood of human–snake interactions and envenomation events [3]. Traditional antivenom therapies, largely unchanged for over a century, are limited by low toxin specificity, frequent adverse reactions, and inadequate neutralization of local tissue damage. In contrast to the well-studied effects of venom toxins, the biological response to antivenom and the mechanisms underlying its side effects remain poorly understood [4, 5].

Snake venoms are complex mixtures of biologically active proteins and peptides that account for approximately 90–95% of the dry venom mass [6]. Several major toxin families dominate the composition of many snake venoms and represent important pharmacological targets for toxin-

neutralizing therapies. Among the most prominent are phospholipases A_2 (PLA_2s), snake venom metalloproteinases (SVMPs), snake venom serine proteases (SVSPs), and three-finger toxins (3FTxs) [9]. Envenomation by snakes generally produces three principal clinical syndromes: haemotoxic manifestations, such as hemorrhage and disturbances of blood coagulation; neurotoxic manifestations, including paralysis of skeletal muscles; and cytotoxic effects, which often lead to localized tissue destruction and necrosis [10, 11].

Haemotoxicity is particularly characteristic of envenomations caused by snakes belonging to the family *Viperidae*. In these cases, the pathological effects are mainly associated with the activity of venom metalloproteinases, serine proteases, and phospholipases A_2 [12,13]. Snake venom metalloproteinases are especially well known for their ability to induce hemorrhage and disrupt several components of the coagulation system, producing a combination of systemic bleeding and impaired clot formation in both prey and human victims [14, 15].

The mechanism of SVMP-induced hemorrhage has been described as a multistep process [16, 17]. During the initial phase, these enzymes degrade structural proteins of the basement membrane and components of the endothelial cell–matrix interface, compromising the structural stability of capillary vessels. In the subsequent phase, endothelial cells detach from the damaged basement membrane and become markedly attenuated, ultimately resulting in rupture of the capillary wall and extravasation of blood into surrounding tissues. In addition to their direct proteolytic activity, SVMPs also contribute to hemostatic disturbances through interference with the coagulation cascade, thereby intensifying hemorrhagic complications [18].

While SVMPs are mainly responsible for microvascular structural degradation, phospholipase A_2 (PLA_2) enzymes contribute significantly to venom-induced toxicity by disrupting cellular membranes and promoting inflammatory responses. PLA_2 catalyzes the hydrolysis of membrane phospholipids, leading to the release of arachidonic acid and subsequent production of pro-inflammatory mediators. In the context of envenomation, PLA_2 activity is associated with myotoxicity, edema formation,

platelet dysfunction, and indirect effects on coagulation pathways, which may cause local tissue damage and systemic complications [19, 20].

Snake venoms therefore have the capacity to modulate coagulation in opposing ways, either accelerating clot formation or impairing it entirely [21]. Coagulopathy represents one of the most significant contributors to morbidity and mortality in snakebite victims. This condition may arise directly from the toxic activity of venom components or from secondary physiological disturbances triggered during envenomation. Numerous venom proteins can act as potent procoagulants, activating the coagulation cascade *in vivo*. However, instead of causing extensive thrombosis, this activation more commonly leads to depletion of clotting factors. The resulting consumption coagulopathy manifests clinically as systemic anticoagulation and an increased risk of bleeding complications [22].

Conventional treatment of snakebite relies on antivenom therapy, which remains the only specific treatment currently available. Despite its life-saving potential, antivenom therapy has several limitations, including limited availability in many regions, the requirement for intravenous administration in clinical settings, and the possibility of adverse reactions associated with heterologous immunoglobulins [23].

In recent years, increasing attention has been directed toward small-molecule enzyme inhibitors as potential adjunct or alternative therapeutic strategies for snakebite envenomation. Metalloproteinase inhibitors such as marimastat have demonstrated the capacity to neutralize SVMP activity and reduce hemorrhagic damage in experimental models [24]. Similarly, the phospholipase A_2 inhibitor varespladib has shown broad inhibitory activity against venom PLA_2 enzymes and protective effects in animal models of envenomation [25, 26].

Although the biochemical and pharmacological effects of these inhibitors have been investigated in several experimental studies, their systemic impact on venom-induced pathology remains incompletely understood, particularly when evaluated through integrated analyses of hematological parameters, coagulation disturbances, and histopathological changes in internal organs. Such combined approaches are essential for understanding the complex pathophysiological mechanisms

underlying viper envenomation and for assessing the therapeutic potential of enzyme-targeting inhibitors.

Therefore, the present study aimed to investigate the histopathological alterations and hematological and coagulation disturbances induced by *Macrovipera lebetina obtusa* envenomation and to evaluate the effects of selected experimental inhibitors targeting major venom enzyme families. By integrating blood analyses with multi-organ histopathological examination, this work seeks to provide new insights into the mechanisms of vipers' venom-induce systemic injury and the potential role of enzyme inhibition as an adjunct strategy for snakebite treatment.

2. Material and methods

2.1 Equipment and reagents

Auto Hematology Analyzer URIT-3000Vet Plus was used for CBC; for coagulation testing - Wondfo Optical Coagulation Analyzer (OCG-102) along with the Prothrombin time reagent kit (PT and International Normalized Ratio (INR)) and Activated Partial Thromboplastin Time reagent kit (APTT). Chemicals for buffers and solutions, buffered formalin, xylene, ethanol were obtained from Medisar LLC (Armenia).

2.2 Snake venom, animal ethics and maintenance

Crude venom of *Macrovipera lebetina obtusa* was sourced from specimens housed in the serpetarium of the Orbeli Institute of Physiology, National Academy of Sciences (Yerevan, Armenia), vacuum-dried at ambient temperature, and stored in the dark at 4°C until use.

Experimental animals (male outbred non-linear albino mice, 20±2 g; male non-linear Wistar strain rats, 200±10 g, Orbeli Institute of Physiology of NAS RA, Yerevan, Armenia) were acclimatized for a minimum of 1 week before experimentation, with their health monitored daily. All experimental animals were maintained under controlled conditions: a 12-hour light/dark cycle (07:00 to 19:00), stable temperature, and standard feeding. Animals were euthanized after venom injection in

compliance with ethical standards. All experimental procedures were conducted in accordance with the principles of laboratory animal care as approved by the Institutional Animal Care and Use Committee (IACUC) of the L.A. Orbeli Institute of Physiology of NAS RA. The study complied with the European Convention for the Protection of Vertebrate Animals Used for Experimental and Other Scientific Purposes (Directive 2010/63/EU of the European Parliament and the Council, September 22, 2010).

2.3 Animals survival assays via a preincubation mode

The mice were divided into four groups for multi-organ histological analysis: a) healthy control; b) mice injected intravenously with freshly diluted *M. l. obtusa* venom at a lethal dose of 2.5 LD_{50} (2.5 × 18.4 μg) [27], c) were each mouse received an intravenous injection via the tail vein of *Macrovipera lebetina obtusa* venom (MLO) at a dose of 2.5 LD_{50}, pre-incubated with 60 μg of marimastat and d) the same concentrations as marimastat were used for varespladib. Incubation was performed at 37 °C. The mixture was subsequently centrifuged at 3000×g for 5 minutes, and the supernatant was used for injection. The venom was dissolved in physiological saline, while marimastat and varespladib were dissolved in DMSO. The final concentration of DMSO in the injected mixture did not exceed 2.5%. Each mouse received 0.3 mL of the prepared solution containing 2.5 LD_{50} of MLO pre-incubated with the respective inhibitor.

2.4 Hematological and Coagulation Analysis

The rats (200 g) were also divided into four groups to assess hematological and coagulation alterations: a) healthy control; b) rats injected intraperitoneally with freshly diluted *M. l. obtusa* venom at an 2LD_{50} dose (LD_{50} for the i.p. injections is 1.86 ± 0.1 mg/kg); c) were each rat received an intraperitoneal injection of MLO at a dose of 2 LD_{50}, pre-incubated with 965.2 μg of marimastat and d) were each rat received an intraperitoneal injection of MLO at a dose of 2 LD_{50}, pre-incubated with 965.2 μg of varespladib.

Incubation was carried out at 37 °C, followed by centrifugation at 3000×g for 5 minutes. The supernatant was then administered. The venom was dissolved in physiological saline, while the inhibitors were dissolved in DMSO, ensuring that the final DMSO concentration did not exceed 2.5%. Each rat received 0.5 mL of solution containing 2 LD_{50} of MLO pre-incubated with the respective inhibitor.

Blood samples were collected from all rats by cardiac puncture and distributed into EDTA-containing vacutainers for complete blood count (CBC) analysis and sodium citrate tubes for coagulation studies [28]. For coagulation assays, a total volume of 0.5 mL was prepared using a standardized 1:9 citrate-to-blood ratio (50 µL of 3.2% sodium citrate and 450 µL of whole blood) [28]. Tubes were gently inverted to ensure adequate mixing and to prevent clot formation. Hematological parameters were analyzed using a Urit-3000Plus veterinary hematology analyzer, with reference intervals applied according to manufacturer calibration and established literature [29, 30]. Coagulation parameters, including prothrombin time (PT/INR) and activated partial thromboplastin time (APTT), were measured using a Wondfo Optical Coagulation Analyzer (OCG-102), with 20 µL of whole blood used per test.

2.5 Skin Hemorrhage Assay

To assess the skin tissue effects of *M. l. obtusa* venom and the protective action of inhibitors, rats were divided into 3 groups: a) healthy control b) rats injected intradermally with 50 µg of *M. l. obtusa* venom diluted in 100 µL of physiological saline, c) rats received an intradermal injection of 50 µg of MLO, pre-incubated with 60 µg of marimastat, and d) the same concentrations were used for the varespladib group. The mixture was incubated at 37 °C, centrifuged at 3000×g for 5 minutes, and the supernatant was injected. The venom was dissolved in physiological saline, and inhibitors were dissolved in DMSO, with a final DMSO concentration below 2.5%. Each rat received 0.1 mL of the prepared solution containing 50 µg of MLO pre-incubated with the corresponding inhibitor. After 24 hours, the animals were euthanized, and the skin was excised for analysis [31].

2.6 Tissue Processing and H&E Staining for Histopathological Evaluation

In the process of dissection and tissue processing, the classical technique to prepare morphological slides was employed [32]. Samples extracted from organs and skin underwent careful dissection before being delicately embedded in paraplast. Paraffin-embedded tissues were sectioned at a thickness of 2.5 μm using a rotary microtome and mounted onto glass slides for histological analysis. Histopathological evaluation of the heart, lung, liver, kidney, and skin tissues from envenomed animals was performed following standard histological procedures.

At the end of the experimental period (24 h and 7 days), surviving animals were euthanized, and organs were collected and fixed in 10% buffered formalin. Tissue samples were dehydrated through a graded ethanol series (70%, 80%, 90%, 95%, and 100%), followed by xylene clearing and paraffin embedding. Sections were subsequently stained with hematoxylin and eosin (H&E). Microscopic examination and image acquisition were carried out at ×100 and ×400 magnifications using an Olympus BX43 light microscope (Olympus, Japan).

2.7 Statistical analysis

Quantitative data are expressed as mean ± standard error of the mean (SEM). Statistical comparisons were performed using one-way analysis of variance (ANOVA), followed by Dunnett's multiple comparison test to assess differences between experimental groups and the corresponding control group. A two-tailed p-value < 0.05 was considered indicative of statistical significance. All analyses and graphical representations were conducted using GraphPad Prism software (version 8.0.1, GraphPad Software, La Jolla, CA, USA).

3. Results

3.1. Changes in Complete Blood Count following *Macrovipera lebetina obtusa* venom exposure and evaluation of experimental inhibitors

Systemic envenomation by *Macrovipera lebetina obtusa* resulted in pronounced alterations in hematological parameters, particularly affecting erythrocyte-related parameters, including red blood cell count (RBC), hemoglobin concentration (HGB), and hematocrit (HCT). These parameters were analyzed across control, venom-only, and inhibitor-treated groups to evaluate the extent of venom-induced hematological disturbances and the modulatory effects of experimental inhibitors (Table 1; Fig.1). In the venom group, a clear elevation of RBC, HGB, and HCT was observed compared to the control group. This pattern is consistent with the development of hemoconcentration, indicating a relative increase in erythrocyte mass within circulating blood. Such changes are not indicative of increased erythropoiesis but rather reflect acute disturbances in vascular integrity and plasma volume.

In animals treated with marimastat, erythrocyte-related parameters were notably lower compared to the venom-only group and approached values closer to those observed in the control group. This suggests that marimastat partially attenuated the hemoconcentration induced by venom exposure. In contrast, the varespladib-treated group demonstrated persistently elevated RBC, HGB, and HCT levels, remaining closer to those observed in the venom group, indicating a less effective correction of venom-induced hematological disturbances. When comparing the two inhibitor-treated groups, animals receiving varespladib consistently exhibited higher erythrocyte-related values than those treated with marimastat, reflecting a more pronounced hemoconcentration. This difference highlights distinct mechanisms of action between the inhibitors and their differential ability to modulate venom-induced systemic effects.

The observed elevation in RBC, HGB, and HCT in venom-exposed animals can be explained by plasma leakage resulting from increased vascular permeability, a hallmark of viper envenomation. Snake venom metalloproteinases are known to degrade components of the vascular basement membrane and disrupt endothelial integrity, leading to extravasation of plasma. As a consequence, the relative concentration of erythrocytes within the bloodstream increases. The comparatively lower values observed in the marimastat group are likely attributable to its inhibitory effect on snake venom metalloproteinases, which are primary mediators of vascular damage. By limiting endothelial

disruption and reducing plasma leakage, marimastat appears to mitigate the degree of hemoconcentration.

In contrast, varespladib acts primarily as an inhibitor of phospholipase A_2 (PLA_2). Although PLA_2 enzymes contribute to cytotoxicity and inflammatory responses, they are not the principal drivers of vascular basement membrane degradation. Therefore, inhibition of PLA_2 alone does not sufficiently prevent vascular leakage, which explains the persistence of elevated RBC, HGB, and HCT values in the varespladib-treated group.

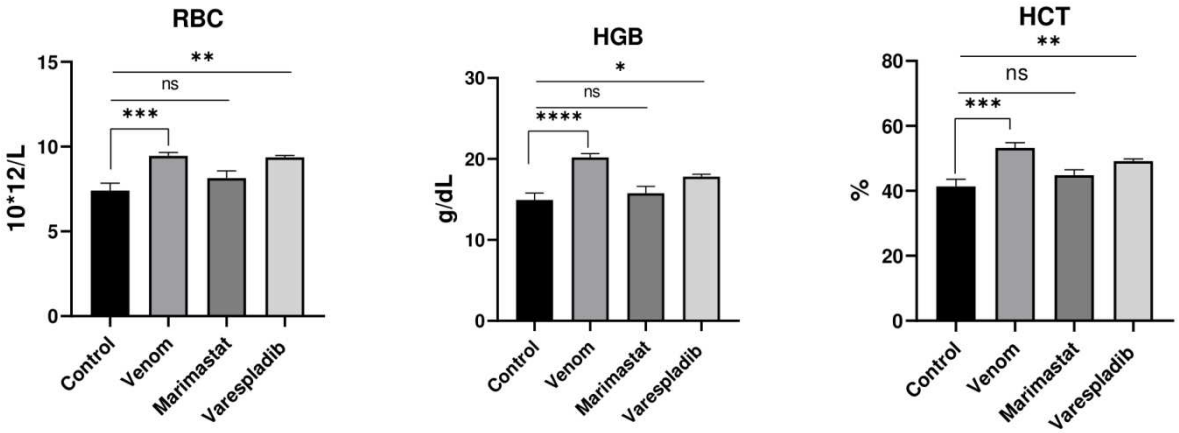


Fig.1. RBC, HGB, HCT levels after the intraperitoneal administration of PBS (Control), Venom, MLO+Marimastat and MLO+Varespladib (experimental repeats–6, mean ± SEM; one-way ANOVA with Dunnett's multiple comparison test, $p^* < 0.05$).

Importantly, other erythrocyte indices such as MCV, MCH, and MCHC remained relatively stable across all groups, indicating that the observed changes were not associated with structural alterations of erythrocytes. Instead, these findings support the interpretation that venom-induced hematological changes are primarily driven by alterations in plasma volume rather than intrinsic red blood cell pathology. Overall, these results demonstrate that *M. l. obtusa* venom induces significant hemoconcentration, and that inhibition of metalloproteinases by marimastat is more effective in attenuating these effects compared to PLA_2 inhibition by varespladib. These findings underscore the

central role of metalloproteinases in mediating vascular dysfunction and systemic hematological disturbances following viper envenomation.

Table 1. Complete Blood Count (CBC) Parameters Across Experimental Groups (experimental repeats–6, mean ± SEM; one-way ANOVA with Dunnett's multiple comparison test).

Group (*)	Control	Venom	MLO+Marimastat	MLO+Varespladib
WBC 10*9/L (2,9-15,3)	4.95±0.24	3.16±0.21	3.87±0.82	3.68±0.85
LYM % (63,7-90,1)	59.7±3.49	49.4±6.03	66.8±3.97	44.75±4.04
MID % (1,5-4,5)	5.26±1.24	7.23±1.12	5.78±0.32	8.53±0.87
GRAN% (7,3-30,1)	35±3.29	43.3±5.22	27.42±3.94	46.72±3.23
LYM 10*9/L (2,6-13,5)	2.17±0.19	1.32±0.23	2.55±0.77	1.65±0.53
MID 10*9/L (0,0-0,5)	0.41±0.19	0.16±0.03	0.20±0.06	0.22±0.05
GRAN 10*9/L (0,4-3,2)	1.65±0.17	1.35±0.24	0.97±0.19	1.65±0.35
RBC 10*12/L (5,6-7,8)	7.4±0.44	9.46±0.19	8.15±0.39	9.37±0.10
HGB g/dL (12,0-15,0)	14.93±0.85	20.18±0.48	15.75±0.78	17.8±0.28
HCT % (36-46)	41.3±2.2	53.2±1.62	44.83±1.52	49.15±0.62
MCV fL (53-68,8)	56.01±0.83	57.3±0.36	55.37±1.16	52.55±0.75
MCH pg (16-23,1)	20.1±0.35	21.2±0.19	19.27±0.29	18.9±0.40
MCHC g/dL (30-34,1)	36±0.38	37.1±0.41	34.98±0.77	36.03±0.23
RDW_CV % (11-15,5)	10.75±0.2	11.75±0.47	11.50±0.19	11.35±0.32
RDW_SD fL	28.76±0.47	30.95±1.07	30.27±0.82	28.18±0.51
PLT 10*9/L (450-900)	581.6±119.7	525.5±69.35	427.50±104.05	414.33±36.72
MPV fL (5,8-6,9)	5.51±0.22	5.4±0.04	5.90±0.10	5.95±0.08
PDW fL	6.65±0.29	6.7±0.06	7.40±0.14	7.60±0.18
PCT %	0.28±0.07	0.27±0.04	0.22±0.07	0.10±0.02
P_LCR %	3.8±0.84	3.5±0.18	5.80±0.70	5.05±0.41
P_LCC 10*9/L	15±3.62	17.8±3.29	20.67±6.78	7.83±1.38

Abbreviations: WBC - White Blood Cells, **LYM** - Lymphocytes, **MID** - Mid-sized cells (Monocytes, Eosinophils, Basophils), **GRAN** - Granulocytes, **RBC** - Red Blood Cells, **HGB** - Hemoglobin, **HCT** -

Hematocrit, **MCV** - Mean Corpuscular Volume, **MCH** - Mean Corpuscular Hemoglobin, **MCHC** - Mean Corpuscular Hemoglobin Concentration, **RDW_CV** - Red Cell Distribution Width – Coefficient of Variation, **RDW_SD** - Red Cell Distribution Width – Standard Deviation, **PLT** - Platelet, **MPV** - Mean Platelet Volume, **PDW** - Platelet Distribution Width, **PCT** - Plateletcrit, **P_LCR** - Platelet-Large Cell Ratio, **P_LCC** - Percentage of Large Cell Count.

* Between parentheses presented the respective Reference Intervals of Hematological Parameters in Rats [30,31].

3.2. Coagulation Disturbances Induced by *Macrovipera lebetina obtusa* Venom and the Effects of Experimental Inhibitors

This study explored how *M. l. obtusa* venom, alone and following pre-incubation with specific inhibitors, influences blood coagulation in rats. Key coagulation markers—Prothrombin Time (PT), International Normalized Ratio (INR), and Activated Partial Thromboplastin Time (APTT)—were used to monitor changes in the clotting profile. In the control group, APTT, PT, and INR values remained within or close to physiological reference ranges, indicating normal coagulation function.

In contrast, the venom group demonstrated a clear disruption of coagulation homeostasis. While APTT values showed high variability, ranging from normal to extremely prolonged levels in some animals, PT and INR values were consistently elevated compared to controls, reflecting a disruption of coagulation processes.

In both inhibitor-treated groups, APTT values remained within the reference range, suggesting preservation of the intrinsic coagulation pathway. However, PT was prolonged in all animals receiving venom in combination with either marimastat or varespladib, and this was accompanied by elevated INR values, indicating persistent impairment of the extrinsic and/or common coagulation pathway. The marimastat-treated group exhibited moderate prolongation of PT and corresponding increases in INR, whereas the varespladib-treated group demonstrated more pronounced and consistent elevations in these parameters. The comparatively improved coagulation profile in the marimastat group may be attributed to the inhibitory activity of marimastat against snake venom metalloproteinases. Inhibition of SVMP activity by marimastat may therefore contribute to stabilization of vascular integrity,

reducing secondary activation and consumption of coagulation factors. As a consequence, the overall coagulation disturbance appears less pronounced in rats receiving this inhibitor. The varespladib primarily targets phospholipase A_2 enzymes. Although PLA_2 toxins play important roles to inflammatory, cytotoxic venom effects and local tissue injury, they are not the principal drivers of coagulation factor consumption or vascular basement membrane degradation in viper envenomation. Therefore, inhibition of PLA_2 alone may not sufficiently counteract the hemostatic disturbances caused by other venom enzymes, particularly serine proteases and metalloproteinases. As a result, animals treated with varespladib continued to demonstrate more pronounced abnormalities in coagulation parameters.

Overall, exposure to *M. l. obtusa* venom induced a coagulation disturbance primarily reflected by prolongation of PT and increased INR, while APTT remained largely unchanged. Pre-incubation with marimastat partially attenuated these alterations in the PT group, whereas varespladib-treated animals continued to exhibit more pronounced abnormalities in coagulation parameters.

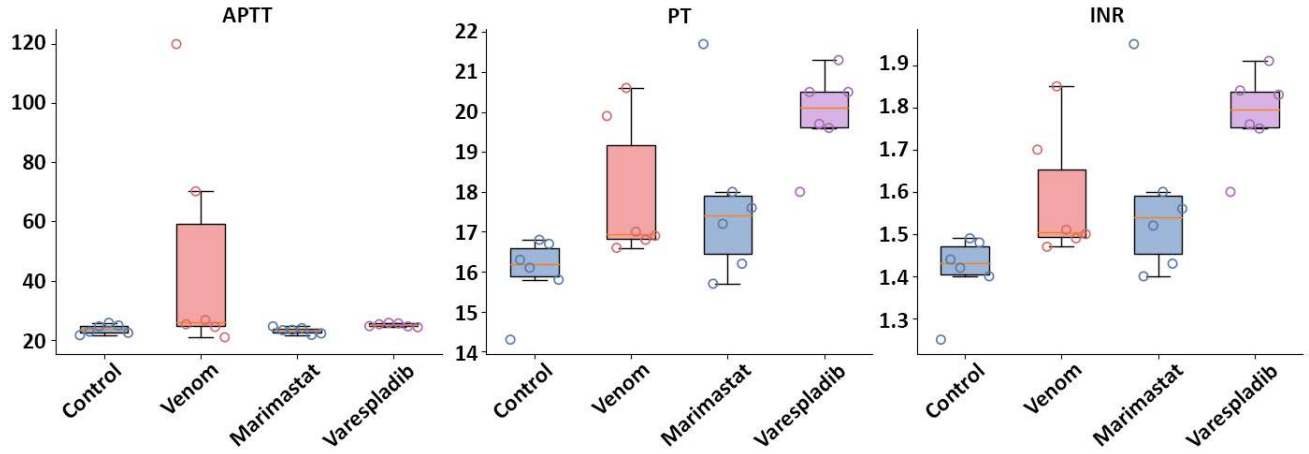


Fig.2. APTT, PT and INR levels after the intraperitoneal administration of PBS (Control), Venom, MLO+ Marimastat and MLO+Varespladib (experimental repeats–6, mean ± SEM; one-way ANOVA with Dunnett's multiple comparison test).

3.3. Organ-Specific Histopathological Changes Induced by *Macrovipera lebetina obtusa* Envenomation: Effects of Experimental Inhibitors

Histopathological examination of tissues revealed distinct morphological changes in mice organs following control, venom and treatment with the experimental inhibitors marimastat and varespladib. The analysis included myocardial, pulmonary, renal, and hepatic tissues obtained from mice, while skin samples were evaluated in rats. Observations were performed at two time points to assess the progression of tissue alterations.

The heart tissue sections of the control group mice had a normal histological appearance. Myocardial muscle fibers were smooth, H&E staining was standard (Fig 3A, 3a, 3E, 3e). In the venom group, myocardial sections demonstrated marked vascular hyperemia, with erythrocyte accumulation in small vessels and the presence of fibrin clots predominantly within veins. Cardiomyocytes exhibited diffuse fragmentation, accompanied by erythrocyte extravasation and hemorrhage formation in multiple myocardial foci (severe hemorrhages, +++) (Fig 3B, 3b, 3F. 3f and Table 2).

In mice treated with marimastat, myocardial sections collected on day 1 demonstrated swelling of cardiomyocytes accompanied by dilation of the intermuscular spaces. Pronounced foci of hemorrhage were observed within the myocardial tissue, and the vessels were markedly hyperemic (severe hemorrhages, +++) (Fig 3C, 3c and Table 2). By day 7, the myocardium remained swollen; however, the hemorrhagic lesions appeared less pronounced and were characterized mainly by moderately expressed foci of hemorrhage (moderate hemorrhages, ++). Despite these alterations, the overall structural organization of the myocardium was preserved, although vascular hyperemia persisted (Fig 3D, 3d and Table 2).

In contrast, mice treated with varespladib, myocardial tissue on day 1 appeared slightly swollen with dilated intermuscular spaces. Weakly expressed foci of hemorrhage (mild hemorrhages, +) were present, and the vessels were hyperemic (Fig 3G, 3g and Table 2). After day 7, the myocardial tissue was mildly edematous with widened intermuscular spaces. Moderately expressed foci of hemorrhage (moderate hemorrhages, ++) were observed, and vascular hyperemia persisted (Fig 3H, 3h and Table2).

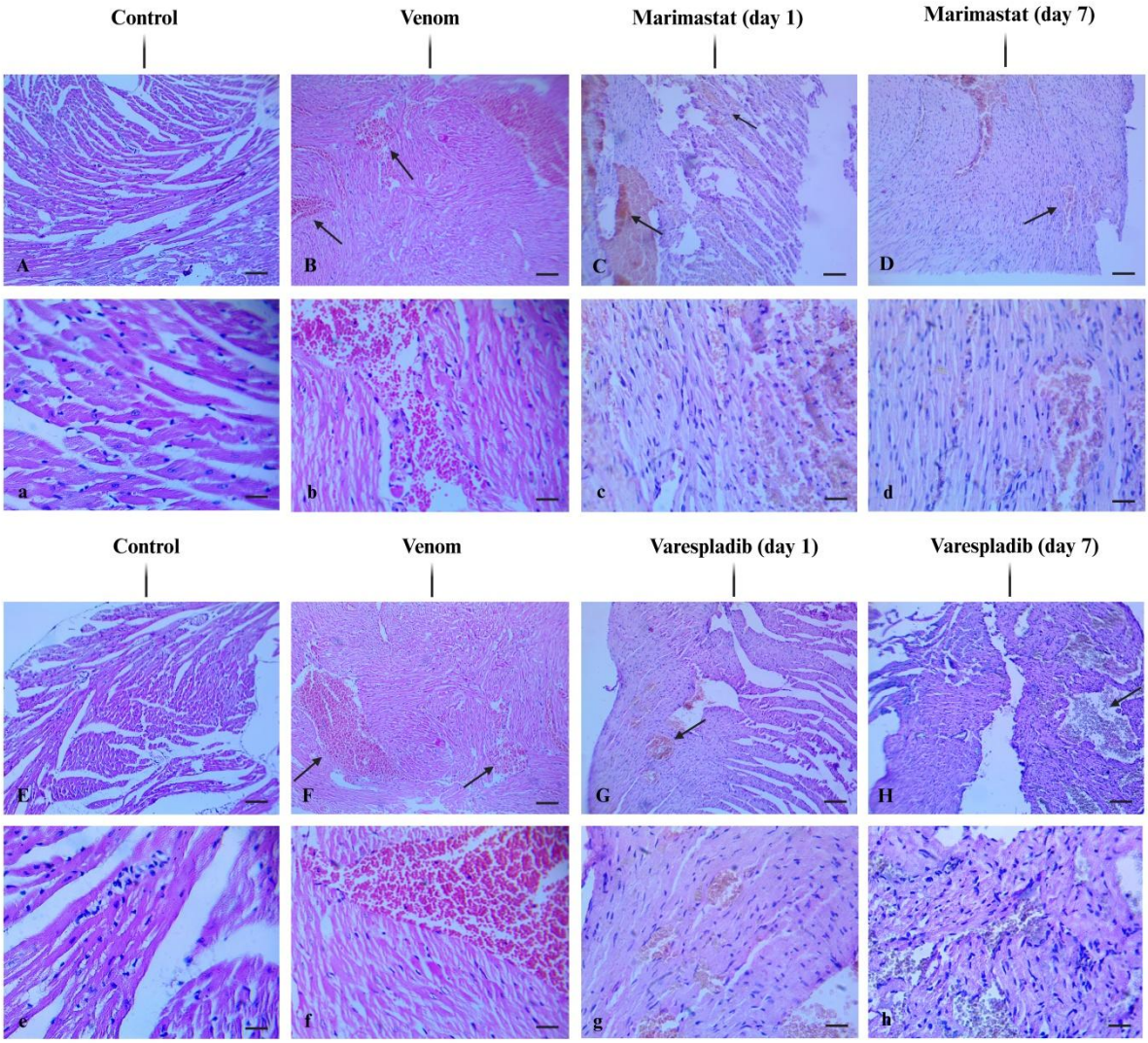


Fig.3. Histopathological changes in cardiac muscles after administration of PBS (Control), Venom, MLO+ Marimastat and MLO+Varespladib. The representative field images were acquired with Olympus BX43. Upper rows: A-D, E-H magnification ×100, scale bar = 250 µm. Lower rows: a-d, e-h magnification ×400, scale bar = 100 µm. Arrows indicate areas of hemorrhages.

In the control group, pulmonary sections demonstrated normal histological appearance, with well-organized bronchi, bronchioles, alveoli, blood vessels, and connective tissue (Fig 4A, 4a, 4E and 4e). In the venom group, lung tissue exhibited marked pathological alterations characterized by vascular changes and severe hemorrhagic involvement. The pulmonary tissue showed pronounced hyperemia due to dilation of alveolar capillaries, with areas of erythrostasis and diapedesis leading to intra-alveolar hemorrhages (severe hemorrhages, +++) (Fig 4B, 4b, 4F, 4f and Table 2).

Lung tissue from marimastat-treated mice showed hyperemia of the pulmonary vessels, accompanied by single foci of intra-alveolar hemorrhage (mild hemorrhages, +) (Fig 4C, 4c and Table 2). Similar findings were observed on day 7, where lung vessels remained hyperemic and isolated intra-alveolar hemorrhagic foci persisted (mild hemorrhages, +) (Fig 4D, 4d and Table 2).

In contrast, varespladib-treated mice exhibited more pronounced pulmonary alterations. Lung vessels appeared markedly hyperemic, and moderately expressed hemorrhagic foci were observed within both the alveolar spaces and stroma (moderate hemorrhages, ++) (Fig 4G, 4g and Table 2). By day 7, severe hyperemic vessels were persisted and moderately expressed hemorrhages (++) were again observed within the stroma and intra-alveolar spaces (Fig 4H, 4h and Table 2).

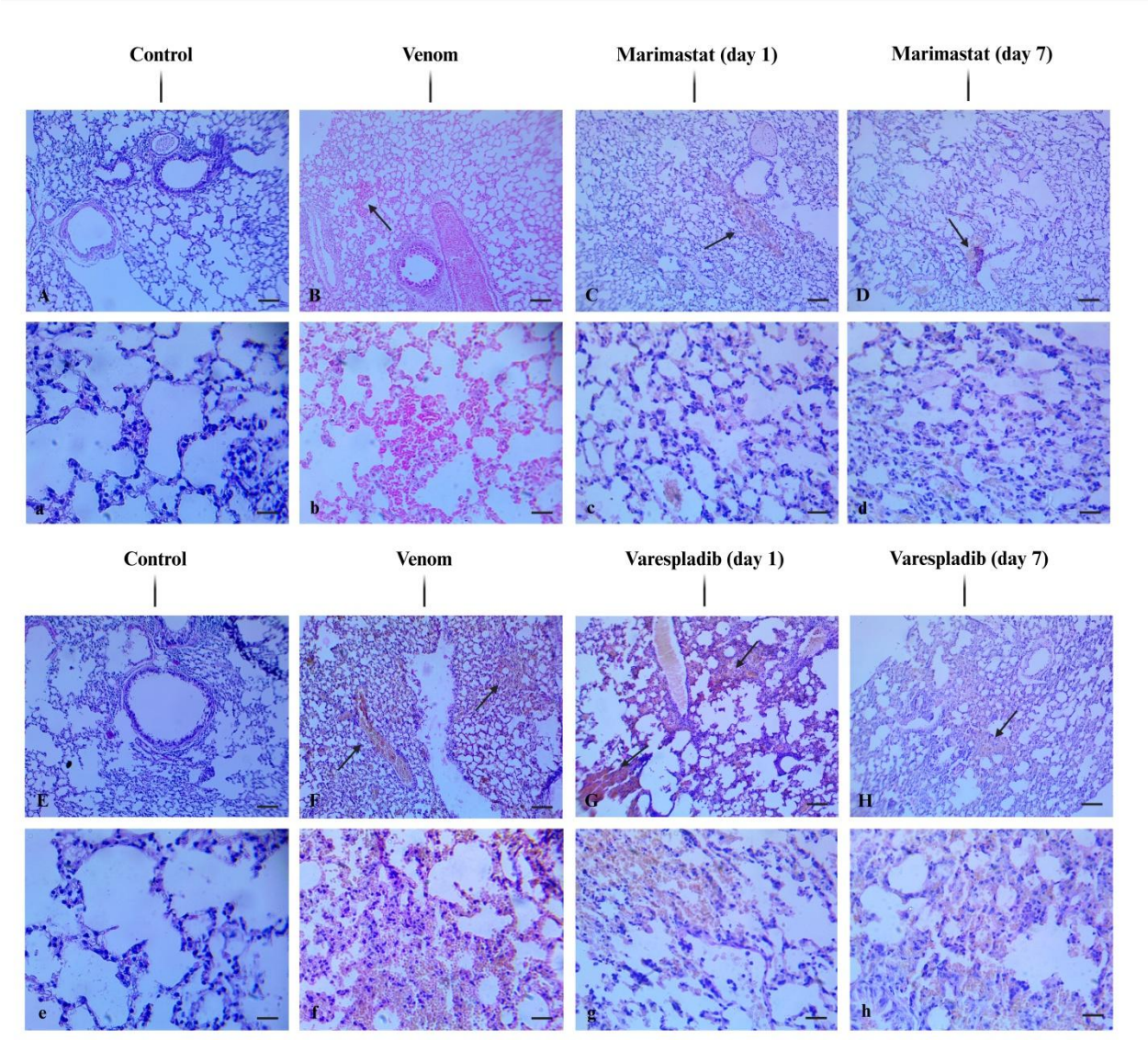
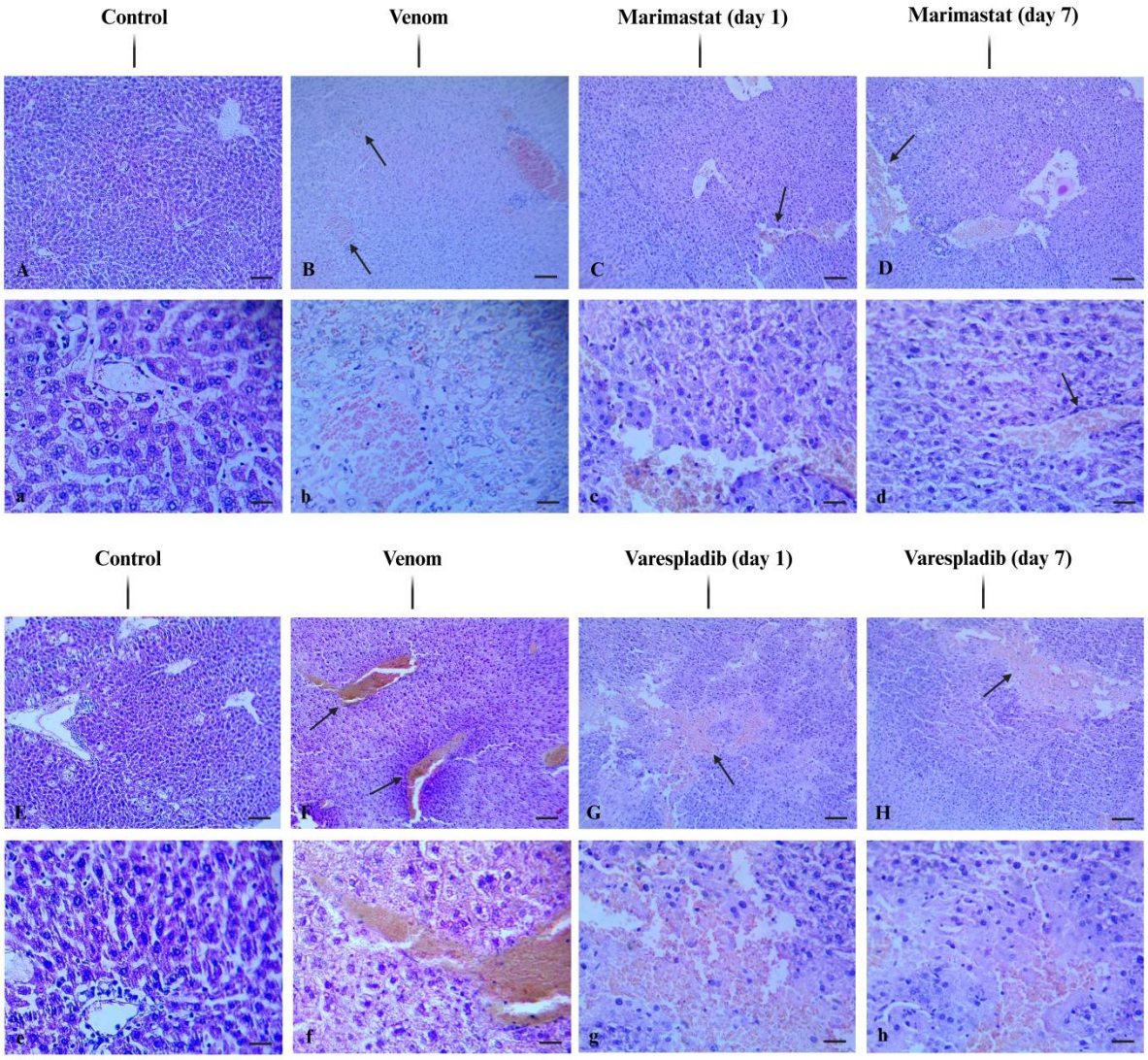


Fig.4. Histopathological changes in lungs after administration of PBS (Control), Venom, MLO+ Marimastat and MLO+Varespladib. The representative field images were acquired with Olympus BX43. Upper rows: A-D, E-H magnification ×100, scale bar = 250 μm. Lower rows: a-d, e-h magnification ×400, scale bar = 100 μm. Arrows indicate areas of hemorrhages

In the control group, liver tissue demonstrated normal histological structure, characterized by well-organized hepatic parenchyma composed of hepatocytes, sinusoidal endothelial cells, and connective tissue structures (Fig. 5A, 5a, 5E, 5e). Liver sections from the venom group demonstrated severe pathological alterations. The hepatic tissue was markedly edematous, with diffuse sinusoidal dilation and extensive areas of hemorrhage. Central veins were dilated and hyperemic, and pronounced vascular congestion with erythrocyte accumulation was observed. In addition, hepatocytes exhibited degenerative changes, including vacuolization and nuclear alterations, while multiple regions showed hepatocellular necrosis, indicating severe tissue injury (severe hemorrhages, +++) (Fig. 5B, 5b, 5F, 5f and Table 2).

Hepatic tissue in the marimastat-treated group appeared moderately swollen. Small foci of hemorrhage were observed within the liver; however, widespread necrotic changes were not detected (mild hemorrhages, +) (Fig 5C, 5c and Table 2). On day 7, hepatic tissue remained edematous and similar small hemorrhagic foci were observed, while the overall architecture of the hepatic parenchyma remained preserved (mild hemorrhages, +) (Fig 5D, 5d and Table 2).

After 1 day the liver sections from varespladib-treated mice demonstrated more severe pathological alterations. The hepatic tissue was markedly edematous and contained extensive areas of hemorrhage. In addition, signs of hepatocyte necrosis were observed in several regions of the liver, indicating more pronounced tissue injury (severe hemorrhages, +++) (Fig 5G, 5g and Table 2). On day 7, hepatic tissue continued to exhibit extensive hemorrhage (+++) and hepatocellular necrosis remained evident, indicating persistent tissue damage (Fig 5H, 5h and Table 2).



370

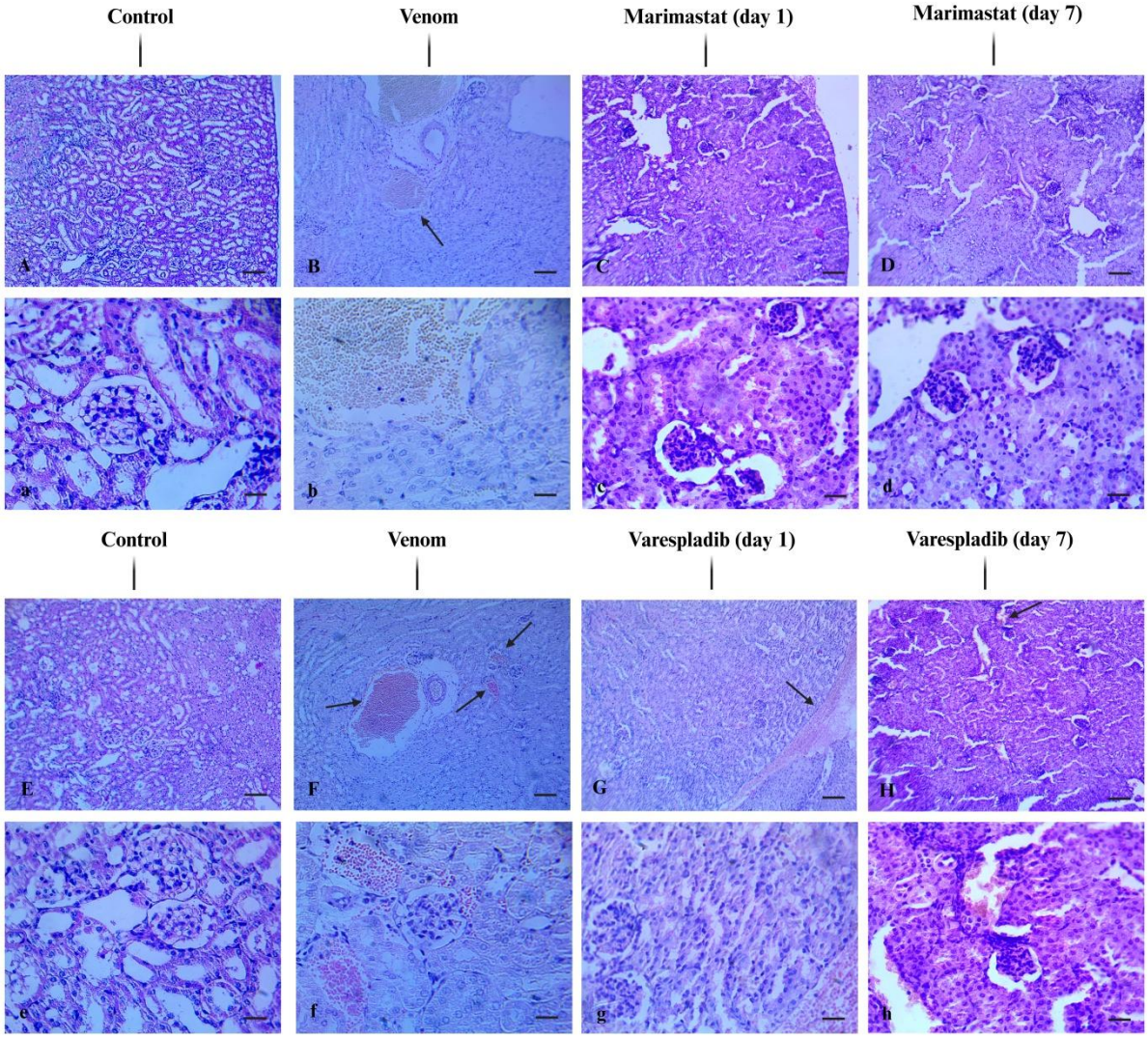
371 **Fig.5.** Histopathological changes in the liver after administration of PBS (Control), Venom, MLO+
372 Marimastat and MLO+Varespladib. The representative field images were acquired with Olympus BX43. Upper
373 rows: A-D, E-H magnification ×100, scale bar = 250 μm. Lower rows: a-d, e-h magnification ×400, scale bar =
374 100 μm. Arrows indicate areas of hemorrhages

375

376 Renal tissue from the control group demonstrated normal histological appearance, with well-
377 defined glomeruli, renal tubules, and interstitial structures (Fig. 6A, 6a, 6E and 6e). In the venom
378 group, kidney tissue exhibited severe pathological alterations, including glomerular swelling, tubular
379 epithelial degeneration, and vascular changes. The tissue was edematous and demonstrated diffuse
380 hemorrhagic foci, indicating extensive vascular involvement (severe hemorrhages, +++) (Fig. 6B, 6b,
381 6F, 6f and Table 2). The kidney from marimastat-treated mice preserved its characteristic

histomorphological organization, comparable to that observed in the control group. The renal parenchyma demonstrated well-defined glomeruli, renal tubules, and interstitial compartments without evident structural disruption. Overall, the kidney sections displayed a histological appearance consistent with preserved renal integrity (Fig 6C and 6c). After 7day renal histology remained within normal limits, with no detectable structural alterations, similar to those observed on the first day (Fig 6D and 6d).

In the varespladib-treated mice, renal tissue on day 1 retained the characteristic histomorphological structure of the kidney; however, moderately expressed hemorrhagic foci (++) were observed in some areas of the renal parenchyma (Fig 6G, 6g and Table 2). After 7 days, the characteristic structure of the kidney is preserved, with a few foci of hemorrhage (mild hemorrhages +) (Fig 6H, 6h and Table 2).



393

394 **Fig.6.** Histopathological changes in the kidney after administration of PBS (Control), Venom, MLO+
395 Marimastat and MLO+Varespladib. The representative field images were acquired with Olympus BX43. Upper
396 rows: A-D, E-H magnification ×100, scale bar = 250 μm. Lower rows: a-d, e-h magnification ×400, scale bar =
397 100 μm. Arrows indicate areas of hemorrhages

398

399 **Table 2.** Tissue damage in some organs: + (mild), ++ (moderate), +++ (severe).

Group	Heart		Lung		Liver		Kidney	
	Day 1	Day 7	Day 1	Day 7	Day 1	Day 7	Day 1	Day 7
Control	-		-		-		-	
Venom	+++		+++		+++		+++	

MLO + Marimastat	+++	++	+	+	+	+	-	-
MLO + Varespladib	+	++	+	+	+++	+++	++	+

400

401 **3.4. Skin Histopathological Changes Following *M. l. obtusa* Envenomation and Inhibitor**
402 **Treatment**

403 Skin sections from the control group demonstrated normal histological structure, with preserved
404 integrity of the squamous epithelium and a well-developed keratin layer. No inflammatory cell
405 infiltration was observed in the subepithelial tissues (Fig. 7A, 7a).

406 In the venom group, the integrity of the squamous epithelium and keratin layer remained preserved;
407 however, the subepithelial tissues were edematous and mildly infiltrated with neutrophils (mild
408 inflammatory reaction, +). Dermal vessels were hyperemic, and small foci of hemorrhage were
409 present (mild hemorrhages, +) (Fig. 7B, 7b and Table 3).

410 In rats treated with marimastat, the squamous epithelium remained intact. The subepithelial tissues
411 were edematous, with a moderately expressed inflammatory reaction (++) characterized by
412 neutrophilic infiltration. Dermal vessels appeared congested, and small foci of hemorrhage were
413 observed (mild hemorrhages, +) (Fig. 7C, 7c and Table 3).

414 In rats treated with varespladib, the overall integrity of the squamous epithelium was also
415 preserved. However, the dermal tissues demonstrated more pronounced vascular alterations, with
416 edema and moderate neutrophilic infiltration (moderate inflammatory reaction, ++). Dermal vessels
417 were markedly congested, and extensive foci of hemorrhage were observed (severe hemorrhages,
418 +++) (Fig. 7D, 7d and Table 3).

419

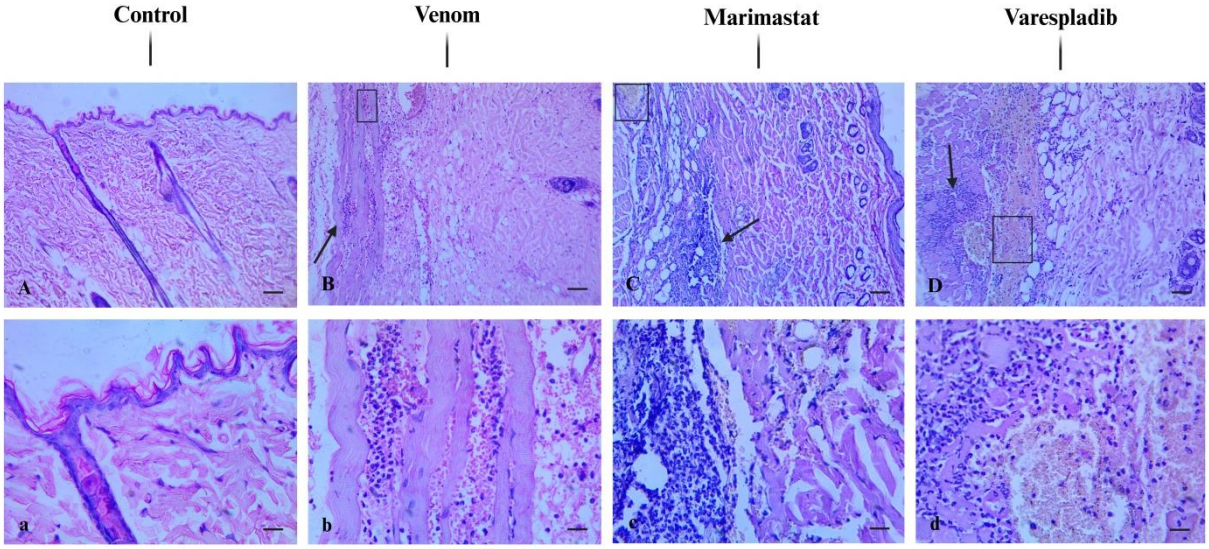
420 **Table 3**. Tissue damage in Skin: + (mild), ++ (moderate), +++ (severe).

Group	***Leukolymphocytic Infiltration***	***Hemorrhage***

Control	-	-
Venom	+	+
MLO + Marimastat	++	+
MLO + Varespladib	++	+++

421

422



423

424 **Fig.7.** Histopathological changes in the skin after administration of PBS (Control), MLO+ Marimastat and
425 MLO+Varespladib. Representative histological sections stained with hematoxylin and eosin (H&E). Upper row:
426 A-D, magnification ×100, scale bar = 250 μm. Lower row: a-d, magnification ×400, scale bar = 100 μm. Square
427 highlights areas of hemorrhage; Arrow indicates leukolymphocytic infiltration.

428

429 **4. Discussion**

430 Coagulopathy induced by *Viperidae* venoms is a complex, multifactorial pathophysiological
431 process in which multiple venom components disrupt normal hemostasis. These venoms contain snake
432 venom metalloproteinases (SVMPs), phospholipases A2, serine proteases (SVSPs), and other
433 bioactive toxins that target coagulation factors, endothelial cells, and platelets, leading to consumption
434 coagulopathy, hemorrhage, and vascular injury [33]. The balance between procoagulant and

anticoagulant venom activities determines whether exposure results in defibrinogenation, disruption of the coagulation pathway, and unpredictable bleeding [10, 17]. Although the clinical manifestations of *Macrovipera lebetina obtusa* envenomation have been described, further clarification of the underlying pathophysiological mechanisms remains essential for improving therapeutic strategies [34, 35].

The findings of the present study clearly demonstrate that venom exposure alone induces pronounced systemic disturbances, which are subsequently modulated but not fully reversed by selective enzyme inhibition. In the venom-only group, a consistent elevation of erythrocyte-related parameters, including red blood cell count, hemoglobin, and hematocrit, was observed compared to controls (Tab. 1). This pattern is most consistent with hemoconcentration rather than increased erythropoiesis, given the short experimental timeframe. These changes reflect acute disturbances in vascular integrity and plasma distribution. Viper venoms are known to increase vascular permeability by degrading endothelial structures and extracellular matrix components, leading to plasma leakage into surrounding tissues. As plasma volume decreases relative to cellular elements, the concentration of erythrocytes increases. Inhibitor-treated groups demonstrated different degrees of modulation of this effect. In the marimastat-treated animals, erythrocyte-related parameters were reduced compared to the venom group and approached control values, indicating partial correction of hemoconcentration. In contrast, the varespladib-treated group maintained elevated erythrocyte indices similar to those observed in the venom group, suggesting that inhibition of phospholipase A_2 alone does not sufficiently prevent venom-induced vascular leakage. These findings highlight the dominant role of metalloproteinases in mediating vascular permeability and plasma extravasation.

The coagulation results further support the presence of venom-induced systemic dysfunction. In the venom-only group, coagulation parameters were clearly disturbed, with consistently elevated prothrombin time and INR, along with marked variability in APTT values (Fig.2). The presence of extreme APTT prolongation in some animals suggests severe and heterogeneous disruption of the coagulation system, likely reflecting differences in toxin distribution and individual susceptibility.

This pattern is consistent with venom-induced consumption coagulopathy, in which clotting factors are activated and subsequently depleted.

In both inhibitor-treated groups, APTT values remained largely within the physiological range, while PT and INR remained elevated, indicating persistent impairment of the extrinsic and common coagulation pathways. However, important differences were observed between the inhibitors. The marimastat group showed comparatively less pronounced coagulation disturbances than the venom group, suggesting partial preservation of hemostatic balance. In contrast, the varespladib group exhibited more consistent and pronounced prolongation of PT and INR, closely resembling the venom-only group. These findings indicate that inhibition of metalloproteinases has a greater impact on limiting coagulopathy than inhibition of phospholipase A_2 alone. This is in line with the known roles of SVMPs, Phospholipase A_2, and SVSPs in directly interacting with coagulation factors and promoting their consumption [36].

Histopathological analysis further confirmed the systemic and organ-specific nature of venom-induced damage. In the venom-only group, all examined organs—including heart, lung, liver, and kidney demonstrated severe hemorrhagic changes, vascular congestion, and structural disruption. These findings are consistent with the central role of metalloproteinases in degrading vascular basement membranes and inducing hemorrhage. Treatment with marimastat resulted in a clear reduction in hemorrhagic severity across most organs. Lung and liver tissues showed only mild hemorrhagic changes, and renal architecture remained largely preserved, indicating effective protection against vascular damage. In contrast, the varespladib-treated group exhibited more pronounced hemorrhagic lesions in several organs, particularly in the liver and lung, where severe hemorrhage persisted. This again suggests that inhibition of PLA_2 does not adequately prevent venom-mediated vascular injury.

A particularly important observation of this study is the distinct behavior of myocardial tissue compared to other organs. In the venom-only group, the myocardium exhibited severe hemorrhagic damage and cardiomyocyte disruption, consistent with combined vascular and cellular injury.

However, the temporal response differed between inhibitor-treated groups. In marimastat-treated animals, myocardial damage was severe at the early time point but decreased to moderate severity by day 7. In contrast, the varespladib group demonstrated mild early changes that progressed to moderate injury over time. This divergence suggests that myocardial injury is not driven solely by vascular damage but also involves direct cellular toxicity. Phospholipase A_2 toxins are known to exert cardiotoxic effects by disrupting cellular membranes, causing calcium imbalance, and inducing mitochondrial dysfunction. Inhibition of PLA_2 by varespladib may therefore reduce early cardiomyocyte injury, explaining the milder initial myocardial changes. However, because metalloproteinase activity persists, vascular and microcirculatory damage continues to develop, leading to progressive injury. Conversely, marimastat does not prevent early PLA_2-mediated cytotoxicity, resulting in more severe initial damage, but by inhibiting metalloproteinases, it limits ongoing vascular injury, allowing partial recovery over time.

Overall, the results of this study demonstrate that the pathological effects of *Macrovipera lebetina obtusa* venom arise from the combined and synergistic action of multiple toxin families. The venom-only group represents the full expression of this toxicity, characterized by hemoconcentration, coagulopathy, and severe multi-organ hemorrhagic damage. Metalloproteinases are the primary drivers of vascular destruction and hemorrhage, serine proteases contribute to coagulation disturbances, and phospholipases A_2 mediate cytotoxic and organ-specific cellular injury.

Selective inhibition of a single toxin class modifies only part of this pathological process. Marimastat provides more effective protection against vascular and hemorrhagic damage and partially attenuates coagulopathy, whereas varespladib reduces early cytotoxic effects but does not adequately control vascular injury or coagulation disturbances. These findings highlight the limitations of single-target therapeutic approaches and support the concept that effective treatment of viper envenomation requires a multi-target strategy that simultaneously neutralizes multiple major toxin families.

Overall, this study provides important insights into the mechanisms underlying venom-induced systemic pathology and demonstrates how selective inhibition of different toxin families influences

hematological, coagulation, and histopathological outcomes. These findings may contribute to the development of more effective therapeutic strategies for snakebite envenomation.

Conclusions

The present study demonstrates that *Macrovipera lebetina obtusa* venom induces complex systemic toxicity characterized by hemoconcentration, coagulopathy, and pronounced multi-organ histopathological damage. The observed prolongation of PT and elevation of INR, together with marked vascular and hemorrhagic alterations across examined tissues, confirm the central role of venom components in disrupting hemostatic balance and microvascular integrity.

Importantly, animals receiving venom pre-incubated with inhibitors survived up to 7 days, demonstrating a substantial reduction in acute toxicity. However, this experimental approach poses a key limitation, as the pre-incubation model does not fully replicate the clinical scenario of snakebite envenomation, in which venom dissemination occurs before therapeutic intervention. Therefore, the translational applicability of these findings requires further investigation in models that more closely mimic real-life envenomation. The differential effects observed between marimastat and varespladib emphasize that targeting a single toxin family is insufficient to fully neutralize the complex pathological mechanisms induced by viper venom. The results support the concept that combined inhibition strategies, targeting multiple toxin classes simultaneously, may yield more effective therapeutic outcomes and should be explored in future studies.

Finally, it is important to consider that snake venom is a highly complex mixture of bioactive components, including metalloproteinases, phospholipases A_2, serine proteases, and other toxins, all of which contribute synergistically to systemic toxicity. A comprehensive therapeutic approach must therefore account for this multifactorial nature of venom action.

Overall, this study provides important insights into the mechanisms of venom-induced systemic injury and highlights the potential and limitations of enzyme-targeting inhibitors as adjunct strategies to improve snakebite treatment.

Declarations

Abbreviations

The following abbreviations are used in this manuscript:

MLO *Macrovipera lebetina obtusa*

SVMP Snake venom metalloproteinases

SVSP Snake venom serin proteases

PLA2 Phospholipase A2

3FTx Three-finger toxins

PT Prothrombin

INR International Normalized Ratio

APTT Activated Partial Thromboplastin Time

CBC Complete Blood Count

RBC Red blood cells

HGB Hemoglobin

HCT Hematocrit

DMSO Dimethyl sulfoxide

EDTA Ethylenediaminetetraacetic acid

Ethics approval and consent to participate

Not applicable.

Consent for publication

All authors have read and approved the final manuscript.

Data availability

The datasets and materials used and/or analyzed during the current study are available from the corresponding author upon reasonable request.

Competing interests

The authors declare no conflicts of interest.

Funding

This study was supported by the Higher Education and Science Committee of the Ministry of Education, Science, Culture and Sports of RA, grant number: 21AG-1F031.

Authors' Contributions

N.A., A.K. and G.A. conceived the investigation. N.A. designed the experiments, G.A. wrote the manuscript. A.A., V.D. & H.K designed and carried out all experiments. All authors have read and agreed to the published version of the manuscript.

References

1. World Health Organization. Snakebite envenoming – A strategy for prevention and control. 2019. Available from: https://www.who.int/publications/i/item/snakebite-envenoming
2. World Health Organization. Target product profiles for animal plasma-derived antivenoms: antivenoms for treatment of snakebite envenoming in sub-Saharan Africa. 1st edition. Geneva: World Health Organization; 2023. Available from: https://www.who.int/publications/i/item/9789240079229
3. Williams DJ, Faiz MA, Abela-Ridder B, et al. Strategy for a globally coordinated response to snakebite envenoming. PLoS Neglected Tropical Diseases. 2019;13(2):e0007059. https://doi.org/10.1371/journal.pntd.0007059

590 4. Brown N, Landon J. Antivenom: the most cost-effective treatment in the world? Toxicon.
591 2010;55(7):1405–7. https://doi.org/10.1016/j.toxi con.2010.02.012
592 5. de Silva HA, Ryan NM, de Silva HJ. Adverse reactions to snake antivenom, and their prevention
593 and treatment. Br J Clin Pharmacol. 2016;81(3):446–52. https://doi.org/10.1111/bcp.12739
594 6. Tasoulis T, Isbister GK. A Review and Database of Snake Venom Proteomes. Toxins (Basel).
595 2017;9(9):290. https://doi.org/10.3390/toxins9090290
596 7. Calvete JJ. Snake venomics: from the inventory of toxins to biology. Toxicon. 2017;75:44-62.
597 https://doi.org/10.1016/j.toxicon.2013.03.020
598 8. Gutierrez JM, Calvete JJ, Habib AG, et al. Snakebite envenoming. Nature Reviews Disease
599 Primers. 2017;3:17063. https://doi.org/10.1038/nrdp.2017.63
600 9. Escalante T, Shannon JD, Moura-da-Silva AM, Gutiérrez JM, Fox JW. Novel insights into
601 capillary damage by snake venom metalloproteinases. Toxicon. 2006;45(8):997-1011.
602 https://doi.org/10.1016/j.toxicon.2005.11.008
603 10. Slagboom J, Kool J, Harrison RA, Casewell NR. Haemotoxic snake venoms: their functional
604 activity, impact on snakebite victims and pharmaceutical promise. Br J Haematol.
605 2017;177(6):947–959. https://doi.org/10.1111/bjh.14591
606 11. Ferraz CR, Arrahman A, Xie C, Casewell NR, Lewis RJ, Kool J, et al. Multifunctional toxins in
607 snake venoms and therapeutic implications: from pain to hemorrhage and necrosis. Front Ecol
608 Evol. 2019;7. https://doi.org/10.3389/fevo.2019.00218
609 12. Hall SR, Rasmussen SA, Crittenden E, Dawson CA, Bartlett KE, Westhorpe AP, et al.
610 Repurposed drugs and their combinations prevent morbidity-inducing dermonecrosis caused by
611 diverse cytotoxic snake venoms. Nat Commun. 2023;14(1):7812.
612 https://doi.org/10.1038/s41467-023-43510-w
613 13. Siigur J, Aaspollu A, Siigur E. Biochemistry and pharmacology of proteins and peptides purified
614 from the venoms of the snakes Macrovipera lebetina subspecies. Toxicon. 2019;158:16–32.
615 https://doi.org/10.1016/j.toxicon.2018.11.294

14. Markland FS Jr, Swenson S. Snake venom metalloproteinases. Toxicon. 2013;62:3–18. https://doi.org/10.1016/j.toxicon.2012.09.004
15. Ayvazyan N, Ghukasyan G, Ghulikyan L, Kirakosyan G, Sevoyan G, Voskanyan A, et al. The contribution of phospholipase A2 and metalloproteinases to the synergistic action of viper venom on the bioenergetic profile of Vero cells. Toxins (Basel). 2022;14(11):724. https://doi.org/10.3390/toxins14110724
16. Gutierrez JM, Rucavado A, Escalante T, Díaz C. Hemorrhage induced by snake venom metalloproteinases: biochemical and biophysical mechanisms involved in microvessel damage. Toxicon. 2005;45(8):997–1011. https://doi.org/10.1016/j.toxicon.2005.02.029
17. Escalante T, Rucavado A, Fox JW, Gutiérrez JM. Key events in microvascular damage induced by snake venom hemorrhagic metalloproteinases. J Proteomics. 2011;74(9):1781–1794. https://doi.org/10.1016/j.jprot.2011.03.026
18. Fox JW, Gutierrez JM. Snake Venom Metalloproteinases. 1st ed. Basel (Switzerland): MDPI; 2017.
19. Ayvazyan N.M., Zaqarian N.A., Ghazaryan N.A., Molecular events associated with Macrovipera lebetina obtusa and Montivipera raddei venom intoxication and condition of biomembranes. BBA–Biomembranes, 2012; 1818(5): 1359-1364. http://dx.doi.org/10.1016/j.bbamem.2012.02.001
20. Kini R.M. (Ed.), Venom Phospholipase A2 Enzymes: Structure, Function and Mechanism, John Wiley & Sons, Chichester, U. K, 1997.
21. Bittenbinder MA, van Thiel J, Cardoso FC, Casewell NR, Gutiérrez JM, Kool J, et al. Tissue damaging toxins in snake venoms: mechanisms of action, pathophysiology and treatment strategies. Commun Biol. 2024;7(1):358. https://doi.org/10.1038/s42003-024-06019-6
22. White J. Snake venoms and coagulopathy. Toxicon. 2005;45(8):951–967. https://doi.org/10.1016/j.toxicon.2005.02.030

641 23. Gutierrez JM, R Casewell N, Laustsen AH. Progress and Challenges in the Field of Snakebite
642 Envenoming Therapeutics. Annu Rev Pharmacol Toxicol. 2025 Jan;65(1):465-485. doi:
643 10.1146/annurev-pharmtox-022024-033544
644 24. Fischer T, Senn N, Riedl R. Design and Structural Evolution of Matrix Metalloproteinase
645 Inhibitors. Chemistry. 2019 Jun 18;25(34):7960-7980. doi: 10.1002/chem.201805361
646 25. Lewin, M.; Samuel, S.; Merkel, J.; Bickler, P. Varespladib (LY315920) Appears to Be a Potent,
647 Broad-Spectrum, Inhibitor of Snake Venom Phospholipase A2 and a Possible Pre-Referral
648 Treatment for Envenomation. Toxins 2016, 8, 248. https://doi.org/10.3390/toxins8090248
649 26. Lewin MR, Gutirrez JM, Samuel SP, Herrera M, Bryan-Quirós W, Lomonte B, Bickler PE,
650 Bulfone TC, Williams DJ. Delayed Oral LY333013 Rescues Mice from Highly Neurotoxic,
651 Lethal Doses of Papuan Taipan (Oxyuranus scutellatus) Venom. Toxins (Basel). 2018 Sep
652 20;10(10):380. doi: 10.3390/toxins10100380
653 27. Kurtović T, Lang Balija M, Ayvazyan N, Halassy B. Paraspecificity of Vipera a. ammodytes-
654 specific antivenom towards Montivipera raddei and Macrovipera lebetina obtusa venoms.
655 Toxicon. 2014;78:103–12. https://doi.org/10.1016/j.toxicon.2013.12.004
656 28. Nielsen VG, Huneke RB, Khan ES. Carbon monoxide releasing molecule-2 enhances
657 coagulation in rat and rabbit plasma. Blood Coagul Fibrinoly sis. 2010;21(3):298–9.
658 https://doi.org/10.1097/MBC.0b013e3283380c88
659 29. Tully TN. Mice and rats. In: Mitchell MA, Tully TN, editors. Manual of Exotic Pet Practice.
660 W.B. Saunders; 2009. p. 326–44. https://doi.org/10.1016/ B978-141600119-5.50015-9
661 30. Car BD, Eng VM, Everds NE, Bounous DI. Clinical pathology of the rat. In: Suckow MA,
662 Weisbroth SH, Franklin CL, editors. American College of Laboratory Animal Medicine. The
663 Laboratory Rat. 2nd ed. Academic Press; 2006. p. 127–46. https://doi.org/10.1016/B978-
664 012074903-4/50008-X
665 31. Avagyan G, Dabaghyan V, Khachatryan H, Aslanyan A, Kishmiryan A, Karapetyan A, et al.
666 (2025) Hematological and coagulation alterations and splenic response following Macrovipera

667 lebetina obtusa envenomation: Evaluation of ovinederived experimental antivenom. PLoS Negl
668 Trop Dis 19(11): e0013724. https://doi.org/10.1371/ journal.pntd.0013724
669 32. Koojevsky D, Gilyarov G, Gilyarov A. Basics of histological technique. 2010.
670 33. Osipov AV, Utkin YN. Snake Toxins Affecting Blood Vessel Walls: Mode of Action and
671 Biological Significance. Int J Mol Sci. 2025;26(19):9439. https://doi.org/10.3390/ijms26199439
672 34. Kazemi, S.M., Al-Sabi, A., Long, C., Shoulkamy, M.I., Abd El-Aziz, T.M., 2021. Case report:
673 recent case reports of levant blunt-nosed viper Macrovipera lebetina obtusa snakebites in Iran.
674 Am. J. Trop. Med. Hyg. 104 (5), 1870–1876. https://doi.org/ 10.4269/ajtmh.20-1640
675 35. Eskafi, A.H., Bagheri, K.P., Behdani, M., Yamabhai, M., Shahbazzadeh, D., Kazemi-
676 Lomedasht, F., 2021. Development and characterization of human single chain antibody against
677 Iranian Macrovipera lebetina snake venom. Toxicon 197, 106–113.
678 https://doi.org/10.1016/j.toxicon.2021.04.017
679 36. Kini RM. The intriguing world of prothrombin activators from snake venom. Toxicon.
680 2005;45(8):1133–1145